Draft version August 3, 2014
Preprint typeset using LaTeX style emulateapj v. 03/07/07

PSA-64 POWER SPECTRUM

Zaki S. Ali[1], Aaron R. Parsons[1,2], Adrian Liu[1], James E. Aguirre[3], David R. DeBoer[2], Daniel C. Jacobs[8], David F. Moore[3], Jonathan C. Pober[4], Jeff Zheng

Draft version August 3, 2014

ABSTRACT

Subject headings:

1. INTRODUCTION

The Donald C. Backer Precision Array for Probing the Epoch of Reionization (PAPER) is a dedicated experiment to measure the power spectrum of highly redshifted 21 cm emission during the Epoch of Reionization. PAPER is but one experiment that aims to detect this faint signal. Other telescopes that have the same goal are the Giant Meter-wave Radio Telescope (GMRT), the LOw Frequency ARray (LOFAR), and the Murchison Widefield Array (MWA). PAPER currently consists of 128 dual-polarization antennae in a 100-200MHz band out in the Karoo desert in South Africa.

The current best upper limit on 21 cm signal level is at $(41mK)^2$ which was measured by PAPER. This limit was acheived by using the delay-spectrum technique to remove foregrounds and by using a maximum redundancy array to essentially measure the same k-modes repeatedly, boosting sensitivity. In this analysis we employ the same techniques mentioned as well is introduce an optimal fringe-fringe rate filter to boost sensitivity and make use of precise calibration via the Omnical redundant calibrator package.

The paper is outlined as follows. In section **??** we describe the observations used in this analysis. In **??** we discuss the improvements in this pipeline with respect to the previous analysis of PSA-32 **?**. We then move on to the data analysis pipeline in section **??**. Seciton **??** describes the results of our efforts and provides new contraints on EoR. We conclude in **??**.

2. OBSERVATIONS

?? Here, we describe the features of the data set used in this analysis. Currently, PAPER boasts a modest 128 dual-polarization antenna array, which was followed by a 64 antenna array. This paper focuses on the latter. We used a maximally redundant configuration of the PAPER array (see Figure 1 for this analysis, relying on all of the redundant baselines for the calibration procedure, but only using a subset of the baselines for the power spectrum analysis. The columns are separated by 30 meters and the rows by 5 meters. For the power spectrum analysis we are using the baselines that correspond to the width between two columns (e.g. 49-41) as well as those that correspond to over and up and down one antenna (e.g. 10-41 and 10-58, respectively). These 154 baselines are instantaneously redundant and therefore they measure the same Fourier modes on the sky. Within a single group of the three types of baselines above, the measurements add coherently, where between groups they add in quadrature. Having repeated measurements of the same baseline type greatly increases sensitivity.

The observation of this 64 antenna data set spanned a 135 day period that commenced on 2012 November 8 (JD62456240) and ended 2013 March 23 (JD62456375). Each baseline instantaneously measured the 100-200 MHz band which was divided into 1024 frequency channels of resolution 97.66 kHz and integrated for 10.7 seconds. In this analysis we analyze observations that spanned, in local siderial time (LST), a range of 1:00 to 10:00 hours. This range corresponds to the "EoR cold patch", in which galaxtic synchrotron power is minimal (away from the center of the galaxy).

3. SUMMARY OF IMPROVEMENTS FROM PSA32

In comparison to the previous PAPER pipeline (see **?**), this analysis took a slightly different approach which included some important steps to improve our bottom line. In short, the improvements included using a new, refined redundant calibration method (Zheng 2014), increasing the width of the wideband delay filter that removes smothe spectrum foregrounds, weighting the lst binned data sets, and optimal fringe rate filtering. In section **??**, we dicuss each of the improvements in more detail.

Figure **??** (TBD) shows the power spectra when each of the steps mentioned above are turned off and for the one where all of them are turned on. We can see the gradual improvement of the power spectra (hopefully).

4. ANALYSIS

Describe the overall flow of the data through of the pipeline. Here we describe the analysis pipeline of the data set obtained in 2012/2013 observing season. Data was first run through a preprocessing compression pipeline which reduces the volume of the data by a factor of forty. Afterwards we calibrate the relative phases of our array on the basis of redundancy using a logcal approach in delay space, and then get the absoultue phase calibration by fitting. We then set the flux scale of our observations by using Pictor A. The logcal done above was a rough estimate of the phase calibration and hence we used Omnical to get the calibrations to higher accuracy. This was a major difference in the pipeline from previous iterations on PAPER data. We then remove foregrounds using the delay filtering technique and form power spectra. The detalis of the above are discussed below and figure **??** shows a block diagram of the analysis

[1] Astronomy Dept., U. California, Berkeley, CA
[2] Radio Astronomy Lab., U. California, Berkeley, CA
[3] Dept. of Physics and Astronomy, U. Pennsylvania, Philadelphia, PA
[4] Physics Dept. U. Washington, Seattle, WA
[8] School of Earth and Space Exploration, Arizona State U., Tempe, AZ

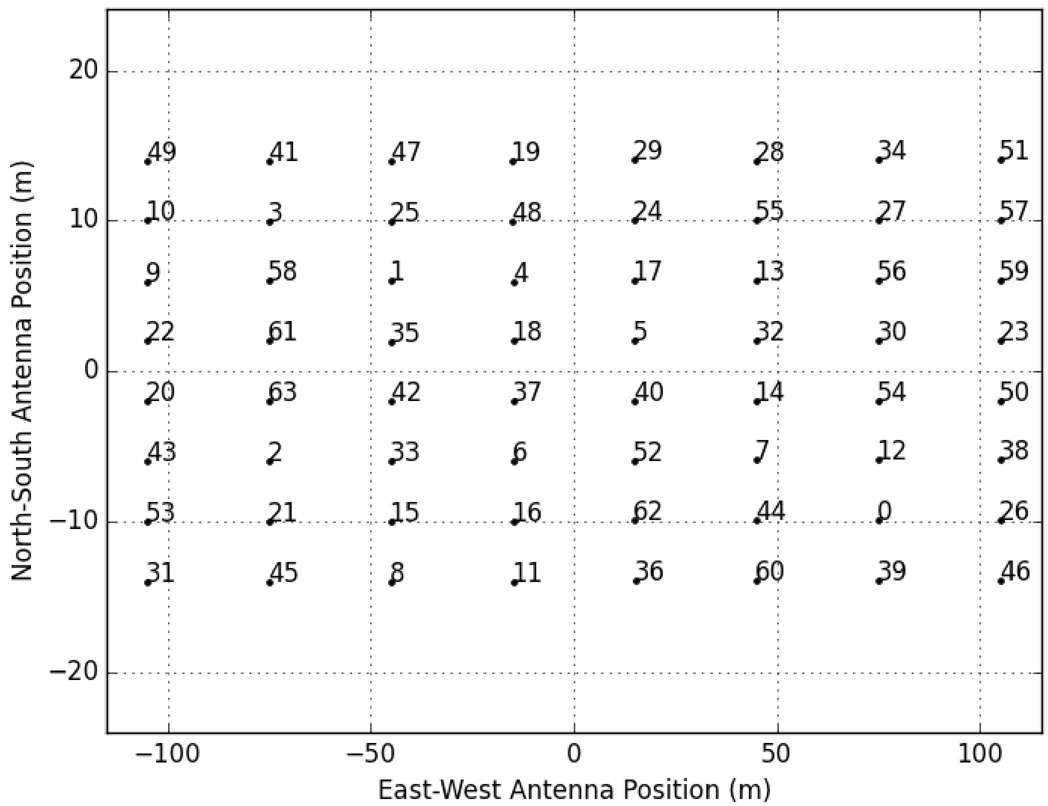

FIG. 1.— Antenna positions for the PAPER 64 observation run.

pipeline.

4.1. *Preprocessing Compression*

As low frequency interferometer grow bigger, data volume becomes an issue. For this data set a 10 minute file consisting of 1024 channel complex visibilites integrated for 10.7 seconds each, requires 4G of storage space. For the observing season this requires about 40TB of storage space. This is doable, for now, but when it comes to analyzing sorting through this much data can be cumbersome. Therfore we have implementd a compression techinque which reduces the amount of storage by a factor of forty. Details of this critical step are presetned in the appendix A of (Parsons et al. 2014). The punch line is that after RFI flagging, and removing unsmooth and transient emission from the data, we end up with a factor of 20 reduction in data volume, ending up with a total data set that requres 2TB of storage. After compression, it ends up that the orignal 1024 channels get downsampled to 203 channels (still encompassing the 100 MHz) and the 60 time samples per 10 minute file end up as 14 timesamples with an effective integration time of 42.8 seconds.

(Show plot of rraw data and compressed data?)

4.2. *Calibrations*

4.2.1. *Overview*

Precise calibration turned out to be critical in improving our bottom line of our final result. We began the calibration procedure by first using a logarithmic calibration scheme based in redundant measurements ((Liu et al. 2010), (**?**)) as well as using standard interferometric self calibration. We set the flux scale of the observations to Pictor A ((**?**) which has the spectrum

$$S_\nu = 382(\frac{\nu}{150MHz})^{-.76}Jy. \tag{1}$$

We then apply the solutions and run through another round of calibration. We use the methods described in (Liu et al. 2010) and (**?**) to use a linearized redundant calibration. Specifically, we used a pre production version of the Omnical package described in (**?**).

4.3. *The logcal*

Before we begin the fine calibration, we perform the same calibration that was done in (**?**). That is, we use redundncy to do a relative phase[6] calibration between antennas, which removes the electrical delays from cables in the signal path. Due to redundancy, we cal calibrate out all of the per-antennas delays in the signal path relative to two parameters which we call τ_{ns} and τ_{es}. These delays are the relative electrical delays that correspond to baseline delays in the north-ssouth and east-west component for 2 reference baselines (49-10 and 49-41,respectively). The antenna based delay solutions vary as much as a couple nanoseconds day to day when

[6] In actuality, we solve for delays to get around phase wrapping issues. These delays are applied to visibilities as $e^{2\pi i\tau\nu}$

solutions are averaged over hour long timescales withing a day. However, the variations in solutions is worse when only averaging over ten minute time scales. . Therefore need for better calibration is requred. We use self calibration to derive the two unknow parameters, τ_{ns} and τ_{ew}, by using Centaurus A, Fornax A, and Pictor A.

Note that there is no possibility of signal loss (see (**?**)).

4.4. *Gain Calibration*

Gain calibration was derived on the basis of redundancy and self calibration. The phase calibrations described above, simultaneously also calibrated for the gain variation between antennas. Again we can only calibrate to a fiducial antenna (49) whose gain is defined as unity. We then perform a self calibration to set the flux scale to Pictor A whose spectrum is derived in (**?**). We use the same methods describes in (**?**).

Figure **??** shows that dataset beamformed to Pictor A, with log janskies on the y axis and lst on the xaxis for a frequncy of .1 + (120/203)*.1/203. As can be seen, the day to day variation in the formed beam has a fractional spread of about 10%. This shows the stability of the instrument and the well behaved calibration solutions derived above.

4.5. *Omnical*

(How did we know that our calibrations was not good enough? Because of the power spectrum? PSA32? We did beamform data to pictorA and say that vs LST, the beamform matched well day to day with a fractional spread of about 10The 10% spread in the formed beam to Pictor A in figure **??** shows the stability of the solutions over time. However, we wanted to do better. The new element to our calibration pipeline was the use of the omnical package developed at MIT by Jeff Zheng ((**?**)). This calibration pipeline takes redundant calibration one step deeper by performing lin cal, which solves for the unbiased phase and gain solutions.

Omnical performs a logcal first to find biased phase and gain solutions so the solutions are close. lincal, in order to converge, requres a guess of the solutions that are close to the actual value. Logcal delivers this result. Because of the calibration performed above, which was an implementation of logcal, the data requried for lincal was already in hand. Lincal was ran on the data and the solutions were applied to the data.

Figure **??** shows the gain solutions output by omnical.

4.6. *lstbinning*

The Omnical calibration pipeline removes all of the variation between unique baseline types and averages them together, effectively creating a model for what a baseline measures. This is not simulated and is derived from the data. These averaged models are what we use to continue through the analysis pipeline.

The motivation for using these datasets is that they are pre calibrated and have baseline to baseline variation removed from them, including cross talk and other systematics. This is essentially the averaged of what a unique baseline type should measure. This includes RFI events that effect the entire array and sky signal.

We lstbin these data into lst bins of 42.8 seconds over the entire observation.

4.7. *WB delay filtering*

Galactic synchrotron and extragalactic point sources, generally foregrounds, greatly contaminate the EOR signal. They are roughly 9 orders of magnitude (Pober 2013a) above the expected level of EOR and can hide low order RFI events and cross-talk. Therefore, its removal is completeley necessary and required in order to obtain the desired EOR signal. In addition to dominating the EOR signal, foregrounds can corrupt higher-order k modes in the power spectrum measurement from the sidelobes arising from RFI flagging and the finite bandwidth used in the line of sight Fourier transform (corresponding to $k_{\parallel}$).

PAPER uses the delay filtering technique described in (**?**) to remove smooth spectrum foregrounds that mask EOR. This method relies on the fact that for a given baseline, there is a maximum delay a source can be measured at. This maximum delay is given when the source is on the horizon. Since the delay is given by projection of the baseline in the direction of the source, the maximum delay is just the time it takes light to travel the baseline length. Following the technique described in (**?**), the delay transform of a visibility takes the form

$$\tilde{V} = \int W(\nu)S(\nu)V(\nu)e^{-2\pi i\tau\nu}d\nu, \tag{2}$$

where $V(\nu)$ is the visibility measured, $W(\nu)$ is a blackman-harris windowing function and $S(\nu)$ is the weighting function that encodes the flags for the data. Hence, the the fourier transoform of the source spectrum convolves the foruier transform of the visibility. Therfore, this method localizes smooth spectrum sources which have a narrow footprint in delay domain. Luckily, most extragalactic sources and synchrotron radiation have power law spectra.

Using the entire bandwidth increases the degree of foreground separation and is impereative to get the best estimate of foreground isolation. We apply the delay transform defined above to every baseline over the entire 100 Mhz. Figure **??** shows the localization of foregrounds for a 30 meter baseline within the horizon of 100 ns. After the filter is applied we see 3 orders of magintude in reduction of foreground isolation. This is a factor of 6 in powerspectra!

Following the method in (Parsons Backer 2009), we use a CLEAN algorithm to deconvolve out the effects of RFI flags and band edge effects. FRI flags and the band edges have the effect of scattering foreground emission to higher order delay modes which would otherwise be uncontaminated. The implementation of CLEAN is such that it treats the RFI flags as a sampling function in frequency and iteratively fits to the highest point in delay space, and therefore trying to fill in the flagged data in frequency. We restrict these CLEAN components to fall within 100 ns of the horizon limit for a given baseline. This CLEAN model is then subtracted off from the the orignal visibility, leaving us with a filterd visibility.

4.8. *optimal Fringe-rate filter*

Before forming power spectra we need to time average visibilities that measure the same k mode on the sky. This is the best way to combine data because we get a $\sqrt{N}$, where N is the number of samples, gain in sensitivity. This is in oppostion to weighting after forming power spectra, where noise beats down as the $\sqrt{N}$. Rather than a straight averaging in time, we can do better by using a weighted averge. Specifically, we want to upweight samples that have higher signal-to-noise.

This is acheived by applying a carefully crafted filter in fringe rate domain, the fourier dual to time. Different patches on the sky correspond to different fringe rates, for a given baseline and frequency. Maximum fringe rates are found along the equatorial plane where zero fringe rates are found around the poles (sources at the poles do not move through the fringes of a baselines). Sources on the other side of the pole, corresponds to negative fringe rates, because they move through the fringe pattern in the opposite direction. By weighing the fringe rates sampled by a baseline by the beam response of the baseline, gives us the optimal fringe rate filer to use for time averaging. See Parsons/Liu 2014 for a detailed discussion.

We implement the optimal fringe rate filter by first calculating the fringe rate of everypoint on the sky and weighting it the beam of a given baseline, summing along constant fringe rate contours, This is then squared to get the effective sensitivity of each fring rate bin (squaringe the power beam). That is we are upweighting fringe rate bins that have greater signal-to-noise. We then fit a gaussian to the optimal filter to have a smooth function, along with tanh function for to have a smooth cut off at the maximum fringe rate for the given baseline and frequency. Note that this only calculated for a given frequency and scaled to other frequencies, due to the fact that fringe rate scales linearly with frequency via

$$f_{max} = \frac{|\mathbf{b}_{eq}|}{c}\omega_{\oplus}\nu \tag{3}$$

To minimize edge effects in time we fourier transform the optimal fringe rate filter to get the time domain convolution kernel and apply it to each visibility for a given channel and baseline.

The exact implementation of the optimal fringe rate filter, uses a convolution kernel of 400 integrations (should we be??). This has the effect of denoising the data as if it averaged over 4.75 hours with a weigthing function that is the beam weighted fringe rate. For each of the baseline types used (30 m baselines of different orientations).

Since the PAPER beam is 45 degrees, and the array is located at a declination of $-30°$ the fringe rates associated with the low signal to noise (down in the beam) correspond to very high and very low/negative fringe rates. Figure **??** shows a cut of the optimal fringe rate at MHz for a 30 m east west baseline. Therfore, the implemented fringe rate filter removes some sky signal, signal associated with fringe rates outside of the ranges shown in Figure **??**. Figure **??** shows that the applied filter removes sky associated with negative fringe rates and very high fringe rates.

5. RESULTS

6. SCIENCE

7. CONCLUSIONS

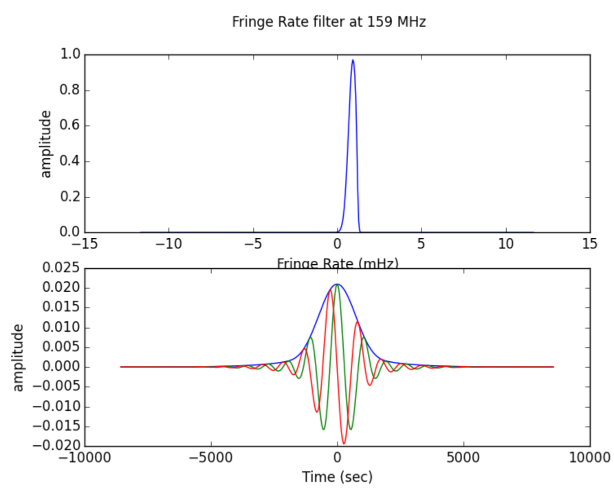

FIG. 2.— slice of a fringe rate filter at a frequency of 159MHz

??

REFERENCES

2004, RocketIO Tranceiver User Guide (UG024 v2.5), Xilinx, http://www.xilinx.com
2005, Virtex-II Pro and Virtex-II Pro X Platform FPGAs: Functional Description (DS083-2 v4.5), Xilinx, http://www.xilinx.com
2006, SKA Demonstrators, Pathfinders and Design Studies EWG Comments on 2006 Updates, SKA Memo 86, Square Kilometre Array, http://www.skatelescope.org/PDF/memos
Baars, J. W. M., Genzel, R., Pauliny-Toth, I. I. K., & Witzel, A. 1977, A&A, 61, 99
Babcock, W. C. 1953, Bell System Technical Journal, 31, 63
Barkana, R., & Loeb, A. 2005a, ApJ, 624, L65
—. 2005b, ApJ, 626, 1
Becker, R. H., et al. 2001, AJ, 122, 2850
Bernardi, G., et al. 2010, A&A, 522, A67+
Bhatnagar, S., Cornwell, T. J., Golap, K., & Uson, J. M. 2008, A&A, 487, 419
Blackman, R. B., & Tukey, J. W. 1958, The measurement of power spectra (Dover Publications Inc.)
Bloom, G., & Golomb, S. 1977, in Proceedings of the IEEE, Vol. 65, 562–570
Bouwens, R. J., et al. 2010, ApJ, 709, L133
Bowman, J. D., Morales, M. F., & Hewitt, J. N. 2006, ApJ, 638, 20
—. 2007a, ApJ, 661, 1
—. 2009, ApJ, 695, 183
Bowman, J. D., Rogers, A. E. E., & Hewitt, J. N. 2008, ApJ, 676, 1
Bowman, J. D., et al. 2007b, AJ, 133, 1505
—. 2013, PASA, 30, 31
Bradley, R. 2006, A Low Cost Screened Enclosure for Effective Control of Undesired Radio Frequency Emissions, NRAO EDIR 317, http://www.gb.nrao.edu/electronics/edir
Bradley, R., Backer, D., Parsons, A., Parashare, C., & Gugliucci, N. E. 2005, in Bulletin of the American Astronomical Society, Vol. 37, 1216–+
Bradley, R., et al. 2008
Brentjens, M. A., & de Bruyn, A. G. 2005, A&A, 441, 1217
Briggs, F. H. 2004, in IAU Symposium, Vol. 217, Recycling Intergalactic and Interstellar Matter, ed. P.-A. Duc, J. Braine, & E. Brinks, 26–+
Brigham, E. O. 1988, The fast Fourier transform and its applications. (Englewood Cliffs, N.J.: Prentice-Hall, 1988)
Burgess, A. M., & Hunstead, R. W. 2006, AJ, 131, 100
Chang, C., Wawrzynek, J., & Brodersen, R. W. 2005, IEEE Design and Test of Computers, 22, 114
Chapiro, D. M. 1984, PhD thesis, Stanford Univ., CA.
Chen, X. 2004, ArXiv Astrophysics e-prints
Chen, X., & Miralda-Escudé, J. 2004, ApJ, 602, 1

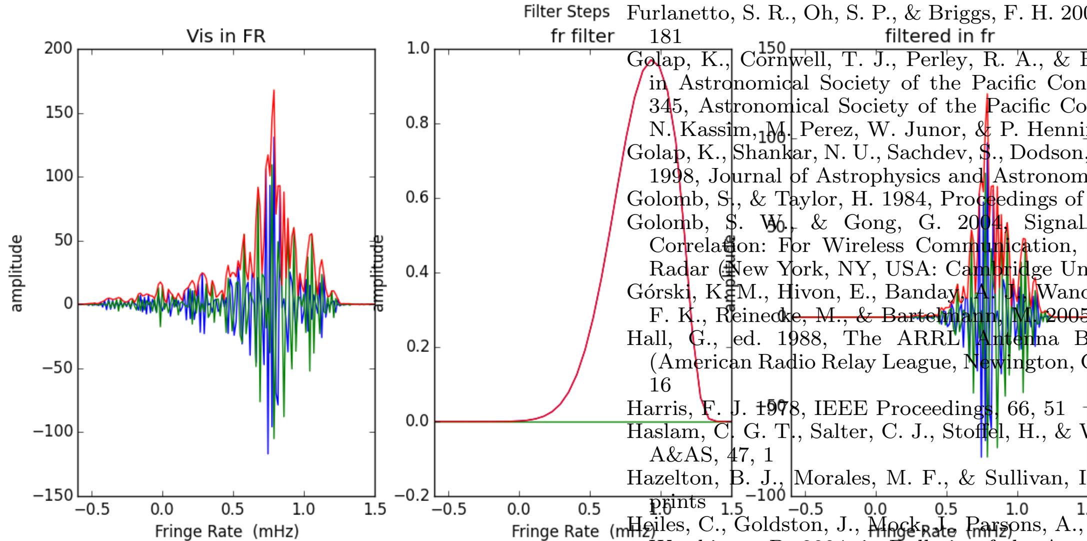

FIG. 3.— slice of a fringe rate filter at a frequency of 159MHz

??

Clark, B. G. 1999, in Astronomical Society of the Pacific Conference Series, Vol. 180, Synthesis Imaging in Radio Astronomy II, ed. G. B. Taylor, C. L. Carilli, & R. A. Perley, 1–+

Comm. for a Decadal Survey of A&A; NRC. 2010, New Worlds, New Horizons in Astronomy and Astrophysics (Natl. Academies Press)

Conway, J. E., Cornwell, T. J., & Wilkinson, P. N. 1990, MNRAS, 246, 490

Cornwell, T., & Fomalont, E. B. 1989, in Astronomical Society of the Pacific Conference Series, Vol. 6, Synthesis Imaging in Radio Astronomy, ed. R. A. Perley, F. R. Schwab, & A. H. Bridle, 185–+

Cornwell, T. J., & Evans, K. F. 1985, A&A, 143, 77

Cornwell, T. J., Golap, K., & Bhatnagar, S. 2003, W-Projection: A New Algorithm for Non-Coplanar Baselines, EVLA Memo 67

Cornwell, T. J., Golap, K., & Bhatnagar, S. 2005a, in Astronomical Society of the Pacific Conference Series, Vol. 347, Astronomical Data Analysis Software and Systems XIV, ed. P. Shopbell, M. Britton, & R. Ebert, 86–+

Cornwell, T. J., Golap, K., & Bhatnagar, S. 2005b, in Astronomical Society of the Pacific Conference Series, Vol. 345, Astronomical Society of the Pacific Conference Series, ed. N. Kassim, M. Perez, W. Junor, & P. Henning, 350–+

Costas, J. 1984, in Proceedings of the IEEE, Vol. 72, 996–1009

Crochiere, R., & Rabiner, L. R. 1983, Multirate Digital Signal Processing (Englewood Cliffs, N.J., Prentice-Hall, Inc., 1983. 336 p.)

D'Addario, L. 2001, Correlators: General Design Considerations, ATA Memo 24, Allen Telescope Array, http://ral.berkeley.edu/ata/memos/

de Oliveira-Costa, A., Tegmark, M., Gaensler, B. M., Jonas, J., Landecker, T. L., & Reich, P. 2008a, MNRAS, 388, 247

—. 2008b, MNRAS, 388, 247

de Villiers, M. 2007, A&A, 469, 793

Demorest, P., Ramachandran, R., Backer, D., Ferdman, R., Stairs, I., & Nice, D. 2004, in Bulletin of the American Astronomical Society, 1598–+

Di Matteo, T., Ciardi, B., & Miniati, F. 2004, MNRAS, 355, 1053

Di Matteo, T., Perna, R., Abel, T., & Rees, M. J. 2002, ApJ, 564, 576

Dick, C. 2000, High-Performance 1024-Point Complex FFT/IFFT V2.0, http://www.xilinx.com

Dillon, J. S., Liu, A., & Tegmark, M. 2013a, Phys. Rev. D, 87, 043005

Dillon, J. S., et al. 2013b, ArXiv e-prints

Dunkley, J., et al. 2008, ArXiv e-prints, 803

Fan, X., Carilli, C. L., & Keating, B. 2006, ARA&A, 44, 415

Field, G. B. 1958, Proc. IRE, 46, 240

Furlanetto, S. R., Oh, S. P., & Briggs, F. H. 2006, Phys. Rep., 433, 181

Golap, K., Cornwell, T. J., Perley, R. A., & Bhatnagar, S. 2005, in Astronomical Society of the Pacific Conference Series, Vol. 345, Astronomical Society of the Pacific Conference Series, ed. N. Kassim, M. Perez, W. Junor, & P. Henning, 366–+

Golap, K., Shankar, N. U., Sachdev, S., Dodson, R., & Sastry, C. V. 1998, Journal of Astrophysics and Astronomy, 19, 35

Golomb, S., & Taylor, H. 1984, Proceedings of the IEEE, 72, 1143

Golomb, S. W., & Gong, G. 2004, Signal Design for Good Correlation: For Wireless Communication, Cryptography, and Radar (New York, NY, USA: Cambridge University Press)

Górski, K. M., Hivon, E., Banday, A. J., Wandelt, B. D., Hansen, F. K., Reinecke, M., & Bartelmann, M. 2005, ApJ, 622, 759

Hall, G., ed. 1988, The ARRL Antenna Book, 15th Edition (American Radio Relay League, Newington, Connecticut, 1988.), 16

Harris, F. J. 1978, IEEE Proceedings, 66, 51

Haslam, C. G. T., Salter, C. J., Stoffel, H., & Wilson, W. E. 1982, A&AS, 47, 1

Hazelton, B. J., Morales, M. F., & Sullivan, I. S. 2013, ArXiv e-prints

Heiles, C., Goldston, J., Mock, J., Parsons, A., Stanimirovic, S., & Werthimer, D. 2004, in Bulletin of the American Astronomical Society, 1476–+

Helmboldt, J. F., Kassim, N. E., Cohen, A. S., Lane, W. M., & Lazio, T. J. 2008, ApJS, 174, 313

Hirata, C. M. 2006, MNRAS, 367, 259

Högbom, J. A. 1974, A&AS, 15, 417

Hui, L., & Haiman, Z. 2003, ApJ, 596, 9

Iliev, I. T., Mellema, G., Pen, U.-L., Bond, J. R., & Shapiro, P. R. 2008, MNRAS, 384, 863

Jackson, T. L., & Farrell, W. M. 2006, Parallel Processing Symposium, International, 44, 2942

Jacobs, D. C., et al. 2011, ApJ, 734, L34

—. 2013, ArXiv e-prints

Jelić, V., Zaroubi, S., Labropoulos, P., Bernardi, G., de Bruyn, A. G., & Koopmans, L. V. E. 2010, MNRAS, 409, 1647

Jelić, V., et al. 2008, MNRAS, 389, 1319

Jenet, F. A., & Anderson, S. B. 1998, PASP, 110, 1467

Jennison, R. C. 1958, MNRAS, 118, 276

Johnson, R. C. 1993, Antenna Engineering Handbook, 3rd Edition (New York, McGraw-Hill, 1993.), 18–23

Keto, E. 1997, ApJ, 475, 843

Komesaroff, M. M. 1960, Australian Journal of Physics, 13, 153

Kuehr, H., Witzel, A., Pauliny-Toth, I. I. K., & Nauber, U. 1981, A&AS, 45, 367

Large, M. I., Mills, B. Y., Little, A. G., Crawford, D. F., & Sutton, J. M. 1981, MNRAS, 194, 693

Lidz, A., Zahn, O., McQuinn, M., Zaldarriaga, M., & Hernquist, L. 2008, ApJ, 680, 962

Liu, A., & Tegmark, M. 2011, Phys. Rev. D, 83, 103006

Liu, A., Tegmark, M., Morrison, S., Lutomirski, A., & Zaldarriaga, M. 2010, MNRAS, 408, 1029

Liu, A., Tegmark, M., & Zaldarriaga, M. 2008, ArXiv e-prints

Loeb, A., & Barkana, R. 2001, ARA&A, 39, 19

Loeb, A., & Zaldarriaga, M. 2004, Physical Review Letters, 92, 211301

Lonsdale, C. J., et al. 2009, IEEE Proceedings, 97, 1497

Madau, P., Meiksin, A., & Rees, M. J. 1997, ApJ, 475, 429

Madau, P., Rees, M. J., Volonteri, M., Haardt, F., & Oh, S. P. 2004, ApJ, 604, 484

Mao, Y., Tegmark, M., McQuinn, M., Zaldarriaga, M., & Zahn, O. 2008, Phys. Rev. D, 78, 023529

Masui, K. W., et al. 2013, ApJ, 763, L20

McQuinn, M., Lidz, A., Zahn, O., Dutta, S., Hernquist, L., & Zaldarriaga, M. 2007, MNRAS, 377, 1043

McQuinn, M., & O'Leary, R. M. 2012, ApJ, 760, 3

McQuinn, M., Zahn, O., Zaldarriaga, M., Hernquist, L., & Furlanetto, S. R. 2006, ApJ, 653, 815

Mesinger, A., Ferrara, A., & Spiegel, D. S. 2013, MNRAS, 431, 621

Mesinger, A., Furlanetto, S., & Cen, R. 2011, MNRAS, 411, 955

Meyer, C., & Papakonstantinou, P. A. 2009, Discrete Appl. Math., 157, 738

Millman, J., & Halkias, C. 1967, Electronic Devices and Circuits (New York, McGraw-Hill, 1967.)

Mirabel, I. F., Dijkstra, M., Laurent, P., Loeb, A., & Pritchard, J. R. 2011, A&A, 528, A149

Mishra, S., Èabriæ, D., Chang, C., Willkomm, D., van Schewick, B., Wolisz, A., & Brodersen, R. 2005, IEEE DySPAN
Moore, D. F., Aguirre, J. E., Parsons, A. R., Jacobs, D. C., & Pober, J. C. 2013, ApJ, 769, 154
Morales, M. F. 2005, ApJ, 619, 678
Morales, M. F., Bowman, J. D., Cappallo, R., Hewitt, J. N., & Lonsdale, C. J. 2006a, New Astronomy Review, 50, 173
Morales, M. F., Bowman, J. D., & Hewitt, J. N. 2006b, ApJ, 648, 767
Morales, M. F., & Hewitt, J. 2004, ApJ, 615, 7
Morales, M. F., & Matejek, M. 2009a, MNRAS, 400, 1814
—. 2009b, MNRAS, 400, 1814
Morales, M. F., & Wyithe, J. S. B. 2010, ARA&A, 48, 127
Noordam, J. E. 2004, in Presented at the Society of Photo-Optical Instrumentation Engineers (SPIE) Conference, Vol. 5489, Society of Photo-Optical Instrumentation Engineers (SPIE) Conference Series, ed. J. M. Oschmann, Jr., 817–825
Ord, S. M., et al. 2010, PASP, 122, 1353
Paciga, G., et al. 2011, MNRAS, 413, 1174
—. 2013, MNRAS
Page, L., et al. 2007, ApJS, 170, 335
Parashare, C. R., & Bradley, R. F. 2009, in 2009 USNC/URSI Annual Meeting
Park, C., Ng, K., Park, C., Liu, G., & Umetsu, K. 2003, ApJ, 589, 67
Parsons, A. 2009, Signal Processing Letters, IEEE, 16, 477
Parsons, A., Pober, J., McQuinn, M., Jacobs, D., & Aguirre, J. 2012a, ApJ, 753, 81
Parsons, A., et al. 2006, in Asilomar Conference on Signals and Systems, Pacific Grove, CA, 2031–2035
Parsons, A., et al. 2008, PASP, 120, 1207
Parsons, A. R., & Backer, D. C. 2009, AJ, 138, 219
Parsons, A. R., Pober, J. C., Aguirre, J. E., Carilli, C. L., Jacobs, D. C., & Moore, D. F. 2012b, ApJ, 756, 165
Parsons, A. R., et al. 2009, Submitted to AJ. ArXiv:0904.2334
—. 2010, AJ, 139, 1468
—. 2014, ApJ, 788, 106
Pearson, T. J., & Readhead, A. C. S. 1984, ARA&A, 22, 97
Pen, U., Chang, T., Hirata, C. M., Peterson, J. B., Roy, J., Gupta, Y., Odegova, J., & Sigurdson, K. 2009, MNRAS, 399, 181
Perley, R. A., Roser, H.-J., & Meisenheimer, K. 1997, A&A, 328, 12
Petrovic, N., & Oh, S. P. 2010, ArXiv e-prints
Plana, L. A., Furber, S. B., Temple, S., Khan, M., Shi, Y., Wu, J., & Yang, S. 2007, IEEE Des. Test, 24, 454
Planck Collaboration et al. 2013, ArXiv e-prints
Pober, J. C., et al. 2011, ArXiv e-prints
—. 2012, AJ, 143, 53
—. 2013, ApJ, 768, L36
Pritchard, J. R., & Loeb, A. 2010, Phys. Rev. D, 82, 023006
—. 2012, Reports on Progress in Physics, 75, 086901
Rabiner, L. R., & Gold, B. 1975, Theory and application of digital signal processing (Englewood Cliffs, N.J., Prentice-Hall, Inc., 1975. 777 p.)
Ricotti, M., & Ostriker, J. P. 2004, MNRAS, 352, 547
Roberts, D. H., Lehar, J., & Dreher, J. W. 1987, AJ, 93, 968
Robinson, J. 1985, IEEE Transactions on Information Theory, 31, 781
Rogers, A. E. E., & Bowman, J. D. 2008, AJ, 136, 641
Rottgering, H. J. A., et al. 2006, ArXiv Astrophysics e-prints
Rybicki, G. B., & Lightman, A. P. 1979, Radiative processes in astrophysics (New York, Wiley-Interscience, 1979. 393 p.)
Santos, M. G., Amblard, A., Pritchard, J., Trac, H., Cen, R., & Cooray, A. 2008, ApJ, 689, 1
Santos, M. G., Cooray, A., & Knox, L. 2005, ApJ, 625, 575
Sault, R. J. 1990, ApJ, 354, L61
Sault, R. J., Teuben, P. J., & Wright, M. C. H. 1995, in Astronomical Society of the Pacific Conference Series, Vol. 77, Astronomical Data Analysis Software and Systems IV, ed. R. A. Shaw, H. E. Payne, & J. J. E. Hayes, 433–+
Schenker, M. A., et al. 2013, ApJ, 768, 196
Shaw, J. R., Sigurdson, K., Pen, U.-L., Stebbins, A., & Sitwell, M. 2013a, ArXiv e-prints
—. 2013b, ArXiv e-prints
Shull, J. M., Stocke, J. T., & Penton, S. 1995, ArXiv Astrophysics e-prints
Sidon, S. 1932, Mathematische Annalen, 106, 536
Slee, O. B. 1995, Australian Journal of Physics, 48, 143
Slurzberg, M., & Osterheld, W. 1961, Essentials of Radio-Electronics, 2nd Edition (New York, McGraw-Hill, 1961.), 595
So, H., Tkachenko, A., & Brodersen, R. 2006, CODES+ISSS
So, K. H. 2007, PhD thesis, Berkeley Wireless Research Center, UC Berkeley, CA.
So, K. H., & Brodersen, R. W. 2006, in 16th International Conference on Field Programmable Logic and Applications (Madrid, Spain), 349–354
Stefan, I. I., et al. 2013, MNRAS
Sullivan, I. S., et al. 2012, ApJ, 759, 17
Switzer, E. R., et al. 2013, ArXiv e-prints
Tanaka, T., Perna, R., & Haiman, Z. 2012, MNRAS, 425, 2974
Tegmark, M. 1997a, ApJ, 480, L87
—. 1997b, Phys. Rev. D, 55, 5895
Tegmark, M., Eisenstein, D. J., Hu, W., & de Oliveira-Costa, A. 2000, ApJ, 530, 133
Tegmark, M., Hamilton, A. J. S., Strauss, M. A., Vogeley, M. S., & Szalay, A. S. 1998, ApJ, 499, 555
Tegmark, M., & Zaldarriaga, M. 2009, Phys. Rev. D, 79, 083530
Thompson, A. R. 1999, in Astronomical Society of the Pacific Conference Series, Vol. 180, Synthesis Imaging in Radio Astronomy II, ed. G. B. Taylor, C. L. Carilli, & R. A. Perley, 11–+
Thompson, A. R., Moran, J. M., & Swenson, Jr., G. W. 2001, Interferometry and Synthesis in Radio Astronomy, 2nd Edition (New York, Wiley-Interscience, 2001. 692 p.)
Tingay, S. J., et al. 2013, PASA, 30, 7
Trac, H., & Cen, R. 2007, ApJ, 671, 1
Vaidyanathan, P. P. 1990, Proc. IEEE, 78, 56
Wang, X., Tegmark, M., Santos, M. G., & Knox, L. 2006, ApJ, 650, 529
Weinreb, S. 1961, Proc. IEEE, 49, 1099
Weinreb, S., & D'Addario, L. 2001, Cost Equation for the SKA, SKA Memo 1, Square Kilometre Array, http://www.skatelescope.org/PDF/memos
White, M., Carlstrom, J. E., Dragovan, M., & Holzapfel, W. L. 1999, ApJ, 514, 12
Wieringa, M. H. 1992, Experimental Astronomy, 2, 203
Wouthuysen, S. A. 1952, AJ, 57, 31
Wright, M. 2005, Real Time Imaging, SKA Memo 60, Square Kilometre Array, http://www.skatelescope.org/PDF/memos
Wrobel, J. M., & Walker, R. C. 1999, in Astronomical Society of the Pacific Conference Series, Vol. 180, Synthesis Imaging in Radio Astronomy II, ed. G. B. Taylor, C. L. Carilli, & R. A. Perley, 171–+
Yatawatta, S., Zaroubi, S., de Bruyn, G., Koopmans, L., & Noordam, J. 2008, ArXiv:0810.5751
Yatawatta, S., et al. 2013, A&A, 550, A136
Yen, J. L. 1974, A&AS, 15, 483
Zahn, O., Lidz, A., McQuinn, M., Dutta, S., Hernquist, L., Zaldarriaga, M., & Furlanetto, S. R. 2007, ApJ, 654, 12
Zaldarriaga, M., Furlanetto, S. R., & Hernquist, L. 2004, ApJ, 608, 622